EMBEDDED FIR GENERALIZED EIGENFILTERS USING TEST INPUTS

Jeffrey O. Coleman

Naval Research Laboratory, Code 5341
Washington, DC 20375
jeffc@alum.mit.edu

ABSTRACT

A systematic approach is proposed for the individual or joint design of FIR filters to meet specifications on either a single filter or an embedding system (possibly multirate). System power gains in response to particular input spectra are optimized using a generalized eigenvector method. Numerical integration is avoided through a time-domain formulation. Real or complex filters with linear or nonlinear phase or N-th band properties are easily handled.

1. INTRODUCTION

The eigenfilter method of FIR-filter optimization of Vaidyanathan and Nguyen [1] and others [2–6] associates the desired optimum filter with the minimum-eigenvalue eigenvector of a positive-definite matrix whose structure embodies the filter specifications. This paper instead uses generalized eigenvectors and eigenvalues of a matrix pair. Both approaches derive conceptually from quadratic optimization and simplify in a test-input framework.

Quadratic optimization of FIR filters begins with linearity. The frequency response $G(\nu) = \sum_n g(n)e^{-j2\pi\nu n}$ of a digital filter is linear in impulse response $g(n)$, and often the latter is linear in underlying variables to be optimized. For example, a linear-phase FIR filter might have an impulse response x_2, x_1, x_0, x_1, x_2 built from optimization variables $\{x_0, x_1, x_2\}$. Mean-square stopband error $\mathrm{MSE}_s = \int_{\mathrm{SB}} |G(\nu)|^2\, d\nu$ is then quadratic in those optimization variables. Mean-square passband error $\mathrm{MSE}_p = \int_{\mathrm{PB}} |G(\nu) - 1|^2\, d\nu$ is similarly quadratic in those variables (with linear and constant terms). (Integrals become means when normalization is added below.) Quadratic designs minimize or constrain such MSEs.

These key MSEs can be rewritten [7]

$$
\begin{aligned}
\mathrm{MSE}_s &= \frac{\int |G(\nu)|^2 S_s(\nu)\, d\nu}{\int S_s(\nu)\, d\nu} \\
\mathrm{MSE}_p &= \frac{\int |G(\nu) - 1|^2 S_p(\nu)\, d\nu}{\int S_p(\nu)\, d\nu}
\end{aligned}
$$

using the binary-valued $S_s(\nu)/\int S_s(\nu)\, d\nu$ and $S_p(\nu)/\int S_p(\nu)\, d\nu$ instead of integral limits. If $S_s(\nu)$ and $S_p(\nu)$ are interpreted as power spectral densities, then MSE_s and MSE_p are input-specific power gains of the test configurations of Fig. 1. (Nonbinary input spectra result in weighted MSEs.) The nature of the optimization is often readily apparent from such test configurations. Requiring

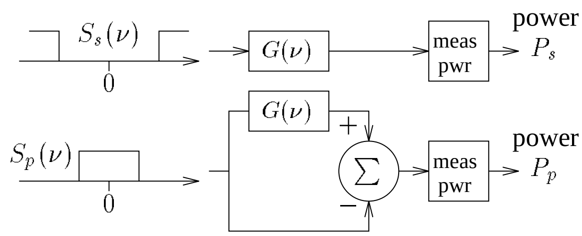

Figure 1: Quadratic optimization of lowpass filter $G(\nu)$ amounts to optimizing the results of these power measurements.

P_s to be much smaller than input power in Fig. 1 forces the filter to reject signals in a stopband corresponding to $S_s(\nu)$, and likewise a small P_p creates a passband by forcing the upper and lower summer inputs to be similar for input spectrum $S_p(\nu)$.

2. THE POWER-GAIN MATHEMATICS

A standard form, presented next, for the impulse responses of a variety of test-system topologies enables subsequent development of a convenient expression for output power. An exact and efficient DFT-based inversion of a broad class of power spectra to obtain the needed autocorrelation samples is then developed.

Concise notation simplifies the presentation. Sequence $h * g$ is the convolution of (scalar, vector, or matrix) sequences h and g, and $(h * g)(n)$ is the value of that sequence at time n. A delayed sequence is denoted with a subscript, so that $g_k(n) = g(n - k)$. Prime $'$ denotes both Hermitian transpose and time reversal, the "match" operation of matched filtering, so that $\mathbf{w}'(n) = \mathbf{w}^H(-n)$. In this notation then, $\langle \mathbf{u}, \mathbf{v} \rangle = (\mathbf{v}' * \mathbf{u})(0)$ concisely expresses the ℓ_2 inner-product vector identity $\langle \mathbf{u}, \mathbf{v} \rangle = \left[\mathbf{v}^H(-n) * \mathbf{u}(n)\right]\Big|_{n=0}$.

2.1. The System Impulse Response

Let vector $\mathbf{x}$ contain the optimization variables, and require any test-system impulse response $h(n)$ dependent on $\mathbf{x}$ to be linear in $\mathbf{x}$, so that $h(n) = \mathbf{x}^T \mathbf{a}(n)$, where $\mathbf{a}(n)$ is the *vector representation sequence* for $h(n)$. Consider the simplest case: If $h(n)$ is FIR with every nonzero element a different real optimization variable, then each corresponding vector in sequence $\mathbf{a}(n)$ is just a different standard unit vector (one nonzero element). From such finite, real, nonlinear-phase sequences it is simple to build responses with more structure. For example, if vector sequences $\mathbf{u}(n)$ and $\mathbf{v}(n)$ have identical support but with distinct unit vectors, sequence $\mathbf{a}(n) = \mathbf{u}(n) + j\mathbf{v}(n)$, or the notationally simpler $\mathbf{a} = \mathbf{u} + j\mathbf{v}$, then represents an arbitrary complex scalar FIR impulse response $g(n) = \mathbf{x}^T(\mathbf{u} + j\mathbf{v})(n)$.

Portions of this work were performed while the author was with Michigan Technological University and were partially supported by National Science Foundation grant MIP-9409686 and Naval Research Laboratory contract N00014-97-P-2030.

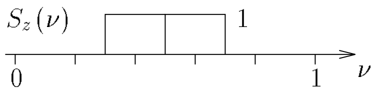

Figure 2: A highpass spectrum in five basis functions per period.

Linear-phase responses are easily specified. Assume for convenience that the support of *basic* finite, real, nonlinear-phase sequences begins at $n = 0$ and that all basic sequences use distinct unit vectors. Using an additional basic vector representation sequence $\mathbf{c}$ of length 1 (representing a delta function of real but indeterminate strength) then, linear-phase impulse response $h(n) = (\mathbf{x}^T\mathbf{a}(n))'_1 + \mathbf{x}^T\mathbf{c}(n) + (\mathbf{x}^T\mathbf{a}(n))_1$ (assume the delay subscript binds more tightly than prime) has vector representation sequence $\mathbf{a}_1^{T\prime}+\mathbf{c}+\mathbf{a}_1$. If $\mathbf{a}$ is basic, then $h(n)$ is a real linear-phase sequence, but if $\mathbf{a} = \mathbf{u} + j\mathbf{v}$ with $\mathbf{u}$ and $\mathbf{v}$ basic, then $h(n)$ is complex.

The identities just used, $\mathbf{x}^T\mathbf{a}+\mathbf{x}^T\mathbf{b} = \mathbf{x}^T(\mathbf{a}+\mathbf{b})$ for sequence addition, $(\mathbf{x}^T\mathbf{a})_k = \mathbf{x}^T\mathbf{a}_k$ for sequence delay, and $(\mathbf{x}^T\mathbf{a})' = \mathbf{x}^T\mathbf{a}^{T\prime}$ for sequence matching, have straightforward counterparts for interpolation, decimation, scaling, catenation, and convolution with a fixed response. They guide computation of vector representation sequences for the impulse responses both of filters with other structural properties (*e.g.*, N-th band) or of quite general test systems.

The Fourier transform of sequence $h(n) = \mathbf{x}^T\mathbf{a}(n)$ is $H(\nu) = \sum_n \mathbf{x}^T\mathbf{a}e^{j2\pi\nu n} = \mathbf{x}^T\mathbf{A}(\nu)$, where $\mathbf{A}(\nu) = \sum_n \mathbf{a}(n)e^{j2\pi\nu n}$ is just the elementwise Fourier transform of vector representation sequence $\mathbf{a}$. (Uppercase $\mathbf{A}(\nu)$ refers here to a vector, not a matrix.)

2.2. Output Power

Begin with perhaps excess generality: suppose $\mathbf{z}(n)$ is a wide-sense-stationary, zero-mean complex vector process, and suppose $\mathrm{g}(n)$ is a complex row-vector impulse response. Then $u = \mathrm{g} * \mathbf{z}$ is a wide-sense stationary zero-mean complex (scalar) process, and the power in u is[1] $E|u|^2 = R_u(0) = (\mathrm{g}*\mathbf{R_z}*\mathrm{g}')(0)$. Further suppose that $\mathrm{g}(n) = \mathbf{x}^T\mathbf{A}(n)$ in terms of complex matrix sequence $\mathbf{A}$. The power in u then becomes[2] $E|u|^2 = \mathbf{x}^T\mathrm{Re}\{(\mathbf{A} * \mathbf{R_z} * \mathbf{A}')(0)\}\mathbf{x}$.

Here vectors g and $\mathbf{z}$ and matrix $\mathbf{A}(n)$ reduce to scalars g and z and column vector $\mathbf{a}(n)$ respectively, so the convolution with the scalar autocorrelation in $E|u|^2 = \mathbf{x}^T\mathrm{Re}\{(\mathbf{a} * R_z * \mathbf{a}')(0)\}\mathbf{x}$ can be moved[3] to obtain the convenient computational form

$$E|u|^2 = \mathbf{x}^T\left(\sum_k \mathrm{Re}\{(\mathbf{a}*\mathbf{a}')(k)R_z^*(k)\}\right)\mathbf{x}. \qquad (1)$$

Only a finite number of autocorrelation samples are required in practice, as the finite length of sequence $\mathbf{a}(n)$ results in a finite sum.

2.3. The Autocorrelation Computation

If the spectrum inverted to obtain $R_z(n)$ is specified in a particular form discussed next, inversion requires an inverse DFT instead of a numerical integral. Even approximating with that spectral form benefits: implicit approximation in the numerical integral is replaced with explicit spectral approximation whose effects are intuitive.

Suppose wide-sense-stationary, complex, random process $z(n)$ has spectral density $S_z(\nu)$ in terms of normalized frequency variable ν or $TS_z(fT)$ in terms of unnormalized frequency f, and suppose $S_z(fT)$, of period T^{-1}, is expressed in a basis comprising frequency-shifted copies of a function $\Phi(NfT)$:

$$S_z(fT) = \sum_k A_k\,\Phi(NfT - k),$$

where sequence A_k has period N. In Fig. 2, a $\{0, 1\}$ valued function $\Phi(\nu)$ supported on $[-0.5, 0.5]$ is used with a sequence A_k of period $N = 5$ to represent a highpass spectrum. A symmetric triangle $\Phi(\nu)$ of width two would yield a piecewise-linear spectrum, a sinc $\Phi(\nu)$ would yield a bandlimited spectrum, etc., and larger N would permit approximation of actual spectra to arbitrary accuracy.

Using a convolution with a periodic impulse train,

$$S_z(fT) = \Phi(NfT) * \sum_k A_k\,\delta\left(f - \frac{k}{NT}\right).$$

Since $NT\,\Phi(NfT)$ and $(NT)^{-1}\sum_k A_k\,\delta(f - k/(NT))$ have inverse continuous-time transforms $\phi(\tau/(NT))$ and[4] $\sum_n a_n\,\delta(\tau - nT)$ respectively, where sequence a_n has period N and is the inverse DFT of sequence A_k, the inverse continuous-time transform of this particular $S_z(fT)$ is

$$R(\tau) = \phi\left(\frac{\tau}{NT}\right)\sum_n a_n\,\delta(\tau - nT).$$

But discrete-time Fourier-transform relationship $R_z(n) \leftrightarrow S_z(\nu)$ ensures that $S_z(fT) = \sum_n R_z(n)e^{-j2\pi fnT}$, implying $R(\tau) = \sum_n R_z(n)\,\delta(\tau - nT)$ because each of the exponentials represents a time-domain delay. Equating these two expressions for $R(\tau)$,

$$R_z(n) = a_n\phi(n/N). \qquad (2)$$

3. THE GENERALIZED EIGENFILTER METHOD

The goal is to minimize an objective function that is some convex[5] combination $\sum_i \alpha_i P_i/R_{z_i}(0)$ of test-system power gains. Input

---

[1] Autocorrelation definition $R_\mathbf{z}(n) = E\left[\mathbf{z}(k)\,\mathbf{z}'(n-k)\right]$ and the identity $(\mathrm{g} * \mathbf{h})' = \mathbf{h}' * \mathrm{g}'$ give $R_u(n) = E\left[(\mathrm{g} * \mathbf{z})(k)(\mathbf{z}' * \mathrm{g}')(n-k)\right] = \sum_{u,v} \mathrm{g}(u)E\left[\mathbf{z}(k-u)\mathbf{z}'(n-k-v)\right]\mathrm{g}'(v) = \sum_{u,v} \mathrm{g}(u)R_\mathbf{z}(n-u-v)\mathrm{g}'(v) = (\mathrm{g} * R_\mathbf{z} * \mathrm{g}')(n)$.

[2] Autocorrelation property $\mathbf{R}'_\mathbf{z} = \mathbf{R_z}$ implies $(\mathbf{A} * \mathbf{R_z} * \mathbf{A}')' = \mathbf{A}'' * \mathbf{R}'_\mathbf{z} * \mathbf{A}' = \mathbf{A} * \mathbf{R_z} * \mathbf{A}'$, so matrix $(\mathbf{A} * \mathbf{R_z} * \mathbf{A}')(0)$ is Hermitian. The $\mathrm{Re}\{\cdot\}$ lowers required storage, with the quadratic in (real) $\mathbf{x}$ unchanged.

[3] If convolution $R_z * \mathbf{a}'$ is commutative, then $(\mathbf{a} * R_z * \mathbf{a}')(0) = ((\mathbf{a} * \mathbf{a}') * R_z)(0) = ((\mathbf{a} * \mathbf{a}') * R'_z)(0) = \sum_k (\mathbf{a} * \mathbf{a}')(k)R'_z(0-k) = \sum_k (\mathbf{a} * \mathbf{a}')(k)R_z^H(k)$.

[4] Write $A(f) = \frac{1}{NT}\sum_i A_i\,\delta\left(f - \frac{i}{NT}\right)$ as

$$A(f) = \frac{1}{NT}\sum_{\substack{k\in[\mathbb{Z}/N\mathbb{Z}]\\ m\in N\mathbb{Z}}} A_k\,\delta\left(f - \frac{k+m}{NT}\right)$$

using a coset decomposition of the integers and using $A_i = A_{k+m} = A_k$. Since $A(f)$ has support in $(NT)^{-1}\mathbb{Z}$ and period T^{-1}, inverse Fourier transform $a(\tau)$ has period NT and support in $T\mathbb{Z}$. For some sequence a_ℓ of period N then, $a(\tau) = \sum_\ell a_\ell\,\delta(\tau - \ell T)$. The area a_n of the time-zero impulse in $a(\tau + nT)$ is the average of its transform $A(f)\,e^{j2\pi fTn}$ over period T^{-1}: $a_n = T\int_{\mathrm{period}} A(f)\,e^{j2\pi fTn}\,df = \frac{1}{N}\sum_{k\in[\mathbb{Z}/N\mathbb{Z}]} A_k \int_{\mathrm{period}} e^{j2\pi fTn}\sum_{m\in N\mathbb{Z}}\delta\left(f - \frac{k+m}{NT}\right)\,df$. Just one impulse is integrated, so $a_n = \frac{1}{N}\sum_{k\in[\mathbb{Z}/N\mathbb{Z}]} A_k\,e^{j2\pi\frac{kn}{N}}$, a periodic sequence and the inverse DFT of sequence A_k.

[5] Condition $\alpha_i \geq 0$ keeps the kernel $\mathbf{Q}_\Sigma$ defined below nonnegative definite. The $\sum_i \alpha_i = 1$ part of the convexity condition is irrelevant.

and output powers of the i-th test system are here designated $R_{z_i}(0)$ and P_i respectively, and (1) showed that P_i has form $\mathbf{x}^T\mathbf{Q}_i\mathbf{x}$, where matrix kernel $\mathbf{Q}_i$ is computed from the particular test-system input autocorrelation $R_z(n)$ (suppressing the "i" subscript) and the vector representation sequence $\mathbf{a}(n)$ (likewise) of the associated test-system impulse response. Autocorrelation samples $R_z(n)$ are computed according to (2). The objective, of form $\mathbf{x}^T\mathbf{Q}_\Sigma\mathbf{x}$, then has straightforwardly computable kernel $\mathbf{Q}_\Sigma = \sum_i \alpha_i \mathbf{Q}_i / R_{z_i}(0)$.

Any test system with an impulse response $\mathbf{x}^T\mathbf{a}(n)$ of the form $\mathbf{x}^T\mathbf{u}(n) - d(n)$ can be accomodated, where the goal is to encourage frequency response $\mathbf{x}^T\mathbf{U}(\nu)$ and frequency response $D(\nu)$ to behave similarly to a degree weighted by test-input spectrum $S_z(\nu)$.

But what is "accomodated"? If $d(n) \neq 0$ for a particular test system, special measures are required. In the test system, multiply $d(n)$ by reference level $G(\nu_0) = \mathbf{x}^T\mathbf{W}(\nu_0)$ to give the test system an impulse response of $\mathbf{x}^T\mathbf{u}(n) - \mathbf{x}^T\mathbf{W}(\nu_0)d(n)$. This reference level is the frequency response at reference frequency ν_0 of some reference system $g(n) = \mathbf{x}^T\mathbf{w}(n)$ linear in the optimization variables. Now it is not simply $D(\nu)$ but $G(\nu_0)D(\nu)$ that $\mathbf{x}^T\mathbf{U}(\nu)$ is to aim for. It might appear that $D(\nu)$ specifies shape while $G(\nu_0)$ specifies level. In fact the effect is to prevent $\mathbf{x}^T\mathbf{U}(\nu)$ from seeking any absolute level, because both are proportional to $\mathbf{x}$. Changing $\mathbf{x}$ to seek a level is not possible when the level moves also. The absolute level of $\mathbf{x}^T\mathbf{U}(\nu)$ and that of $D(\nu)$ are tied together, and the latter is actually determined directly in the optimization.

Recall that ratio α/β and vector ψ are a generalized eigenvalue and the associated generalized eigenvector respectively for the pair of real symmetric matrices $(\mathbf{Q}_\Sigma, \mathbf{V})$ if $\beta\mathbf{Q}_\Sigma\psi = \alpha\mathbf{V}\psi$. If $\beta = 0$, the generalized eigenvalue is infinite. A version of the Rayleigh principle states that $\min_\mathbf{x}\{\mathbf{x}^T\mathbf{Q}_\Sigma\mathbf{x} : \mathbf{x}^T\mathbf{V}\mathbf{x} = 1\}$ is equal to the minimum generalized eigenvalue and that the minimizing vector $\mathbf{x}$ is the associated generalized eigenvector. Here if we set $\mathbf{V}$ to rank-one matrix $\mathbf{W}(\nu_0)\mathbf{W}^H(\nu_0)$ we can solve a generalized eigenproblem to obtain the $\mathbf{x}$ that minimizes quadratic objective $\mathbf{x}^T\mathbf{Q}_\Sigma\mathbf{x}$ subject to the requirement that $|G(\nu_0)|^2 = |\mathbf{x}^T\mathbf{W}(\nu_0)|^2 = 1$, which sets reference level $G(\nu_0)$ to some $e^{j\theta}$.

So the addition of the reference level to the test system is not without effect on the solution, but the effect is minimal. The test-system impulse response is now effectively $\mathbf{x}^T\mathbf{u}(n) - d(n)e^{j\theta}$. If the same reference level is used throughout the design, the effect is to rotate every "desired" response in the entire design, and hence the optimized responses as well, by some unknown θ in the complex plane. That is, the optimization will be able to produce the desired impulse response(s) only up to a complex rotation.

4. EXAMPLES

Two examples, one simple and one more involved, illustrate the concepts. Computation was done in scilab [8] in both cases.

4.1. A Linear-Phase Lowpass Filter

Figure 3 shows the magnitude response of a length-13 real, linear-phase FIR filter optimized by this method. In the optimization the center and right side respectively of its origin-centered impulse response had vector representation sequences $\mathbf{c}(n)$ and $\mathbf{r}_1(n)$, where

$$\begin{aligned}\mathbf{c}(n) &= \mathbf{e}_1\delta(n)\\ \mathbf{r}(n) &= \mathbf{e}_2\delta(n) + \mathbf{e}_3\delta(n-1) + \mathbf{e}_4\delta(n-2)\\ &\quad + \mathbf{e}_5\delta(n-3) + \mathbf{e}_6\delta(n-4) + \mathbf{e}_7\delta(n-5)\end{aligned}$$

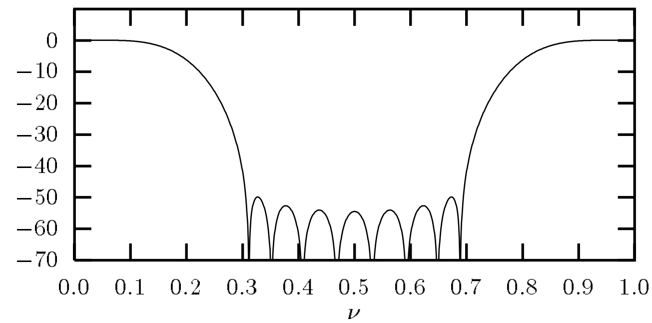

Figure 3: Magnitude response (in dB) of example lowpass filter.

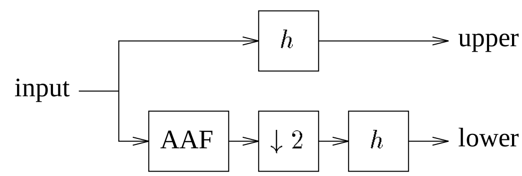

Figure 4: Simple bandsplitting with complex "anti-aliasing" filter AAF and complex FIR filters $h(n)$ at two sampling rates.

and where $\mathbf{e}_i$ is the standard unit vector with unity in the i-th position. The differing unit vectors associated the weights of the different impulses with different optimization variables. (Vector representation sequences $\mathbf{c}(n)$ and $\mathbf{r}(n)$ are basic.) The resulting impulse response had vector representation sequence $\mathbf{g} = \mathbf{r}_1' + \mathbf{c} + \mathbf{r}_1$.

The general scheme of Fig. 1 was used with an objective that summed 95% of the upper-system power gain with 5% of the lower-system power gain, emphasising stopband MSE minimization over passband MSE minimization by a factor of 20. The stopband width was set by the edge frequency of $\nu = 0.3$ for the highpass input spectum in the upper diagram, and the passband width was set by the edge frequency of $\nu = 0.1$ for the lowpass input spectum in the lower diagram. Five rectangular basis functions with appropriate coefficients represented each spectrum, just as in Fig. 2, so the computation with (2) of the 25 autocorrelation samples needed for computation of the 7×7 kernel in (1) required periodic extension of the results of a five-point inverse DFT followed by sinc scaling.

The reference level used was the DC response of the filter. The time-symmetric impulse-response structure of this linear-phase filter guaranteed a real frequency response, so the unknown complex rotation θ given the impulse response by the optimization had to amount to scaling by ± 1. Scaling by -1 in fact resulted and was removed afterwards.

4.2. A Super-Simple Wavelet-Decomposition Bank

The simple system of complex filters of Figure 4 splits off two spectral bands from the input, roughly an upper band $[0.4, 0.8]$ of frequencies passed by the upper filter and the $[0.2, 0.4]$ upper half of the band below, with the latter output at half the input sampling rate. The anti-aliasing filter labeled "AAF" is the lowpass filter designed in the previous example shifted up by 0.3 in frequency by multiplication of its coefficient sequence by the appropriate complex exponential. The two output filters have identical complex impulse responses $h(n)$ of length seven, to be optimized here. (It would be just as easy to do a joint design of two different filters.)

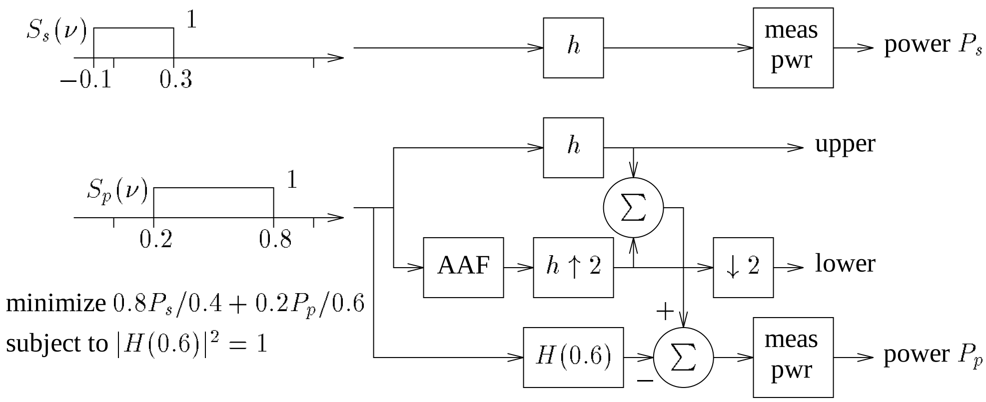

Figure 5: Design specification for filter $h(n)$ of Fig. 4.

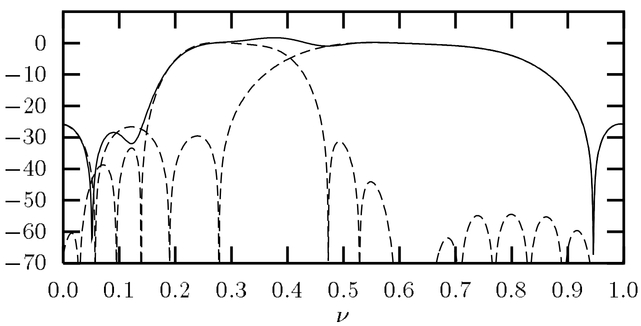

Figure 6: Magnitude responses (in dB) to lower/upper summer inputs (left/right dotted curves) and output (solid curve) in Fig. 5.

Figure 5 shows the complete design specification. An objective that favors stopband MSE control over passband MSE control by 80%/20% is specified. Stopband power gain $P_s/0.4$ is again computed in a single-filter test system but now using an asymmetric input spectrum (of a complex random process) uniformly supported on $[-0.1, 0.3]$. Passband power gain $P_p/0.6$ is computed in a basic system identical to that of Figure 4 except that a Noble identity was used to move the decimator to the right past the lower filter, whose impulse response has been zero-interpolated by two to compensate. If the desired bandsplit is successful, the sum of the two filter outputs (now at the same sampling rate) should pass the combined band $[0.2, 0.8]$. Here the passband gain sought is the reference level $H(0.6)$, the gain of the individual filter at what we expect to be the center of its passband. The passband specification pushes the gain of the entire passband (of the sum filter) towards $H(0.6)$, and the generalized-eigenvalue method constrains this reference level to unit magnitude. Figure 6 shows the optimized magnitude responses of the upper-path filter $h(n)$, the lower-path filters $(\mathrm{AAF} * (h \uparrow 2))(n)$, and their sum.

The optimization set-up begins with the creation of basic vector representation sequences $\mathbf{c}$ of length one and $\mathbf{u}$ and $\mathbf{v}$ of length three. The right side of complex impulse response $h(n)$ then has vector representation sequence $\mathbf{r} = (\mathbf{u} + j\mathbf{v})_1$, and the linear-phase sequence $h(n)$ itself has vector representation sequence $\mathbf{g} = \mathbf{r}' + \mathbf{c} + \mathbf{r}$. The impulse response of the box labeled $H(0.6)$ is $H(0.6)\delta(n)$, where reference level $H(0.6) = \mathbf{x}^T\mathbf{G}(0.6)$. (It would have been just as easy to use the frequency response of the sum, for example.) For stopband power P_s, $R_z(n)$ and $\mathbf{a}(n)$ in (1) become $R_s(n)$ and $\mathbf{g}(n)$ respectively, and for passband power P_p they become $R_p(n)$ and $(\mathbf{g} - \mathrm{AAF} * (\mathbf{g} \uparrow 2))(n) - \mathbf{G}(0.6)\delta(n)$. Spectral inversion is based on rectangular spectral basis functions.

No suggestion is here offered that this is a reasonable filter-bank design. It is simply an example contrived to illustrate the generality of the method.

5. REFERENCES

[1] P . P . Vaidyanathan and Truong Q. Nguyen, “Eigenfilters: A new approach to least-squares FIR filter design and applications including nyquist filters,” *IEEE Transactions on Circuits and Systems*, vol. CAS-34, no. 1, pp. 11–23, Jan. 1987.

[2] Soo-Chang Pei and Jong-Jy Shyu, “Complex eigenfilter design of arbitrary complex coefficient FIR digital filters,” *IEEE Transactions on Circuits and Systems II*, vol. CAS-40, no. 1, pp. 32–39, Jan. 1993.

[3] Truong Q. Nguyen, “The design of arbitrary FIR digital filters using the eigenfilter method,” *IEEE Transactions on Signal Processing*, vol. 41, no. 3, pp. 1128–1139, Mar. 1993.

[4] Soo-Chang Pei and Jong-Jy Shyu, “A unified approach to the design of quadrantally symmetric linear-phase two-dimensional FIR digital filters by eigenfilter approach,” *IEEE Transactions on Circuits and Systems II*, vol. CAS-42, no. 10, pp. 2886–2890, Oct. 1994.

[5] Hong Chen and Gary E. Ford, “A unified eigenfilter approach to the design of two-dimensional zero-phase FIR filters with the mcclellan transform,” *IEEE Transactions on Circuits and Systems II*, vol. CAS-43, no. 8, pp. 622–626, Aug. 1996.

[6] L. Andrew, V. T. Franques, and V. K. Jain, “Eigen design of quadrature mirror filters,” *IEEE Transactions on Circuits and Systems II*, vol. CAS-44, no. 9, pp. 754–757, Sept. 1997.

[7] Rajesh R. Venkatraman and Jeffrey O. Coleman, “A test-waveform view of the quadratic design of FIR filters,” in *Proc. the 7th Int'l Conf. on Signal Processing Applications and Technology (ICSPAT '96)*, Oct. 1996.

[8] Scilab Group, Institut National de Recherche en Informatique et Automatique, Le Chesnay Cedex, France, *Signal Processing With Scilab*, scilab@inria.fr.